https://doi.org/10.46861/bmp.33.014 PŮVODNÍ PRÁCE/ORIGINAL PAPER

Pargasite and forsterite phenocrysts from Očová (central Slovakia)

Pavol Myšľan[1,2]*, Tomáš Bancík[3] and Tomáš Mikuš[4]

[1]Earth Science Institute, Slovak Academy of Sciences, Dúbravská cesta 9, P. O. BOX 106, 840 05 Bratislava, Slovakia; e-mail: *pavol.myslan@savba.sk
[2]Department of Mineralogy, Petrology and Economic Geology, Faculty of Natural Sciences, Comenius University in Bratislava, Ilkovičova 6, Mlynská dolina, 842 15 Bratislava, Slovakia
[3]Slovak Mineralogical Society, Viestova 6623/26, 974 01 Banská Bystrica, Slovakia
[4]Earth Science Institute, Slovak Academy of Sciences, Ďumbierska 1, 974 11 Banská Bystrica, Slovakia

Myšľan P, Bancík T, Mikuš T (2025) Pargasite and forsterite phenocrysts from Očová (central Slovakia). Bull Mineral Petrolog 33(1): 14-19. ISSN 2570-7337

Abstract

The new occurrence of pargasite and forsterite phenocrysts was discovered in basalts in the area of a former field near the Očová village, Zvolen Co., Banská Bytrica Region (central Slovakia). Pargasite forms vitreous dark brown to black crystals up to 6 cm in size. Its chemical composition shows dominant Mg^{2+} (3.07 - 3.16 *apfu*) followed by Fe^{2+} (0.84 - 1.00 *apfu*) and elevated Ti (0.22 - 0.27 *apfu)* at the amphibole crystallochemical *C* site with the average chemical composition (n = 15) $^{A}(Na_{0.58}K_{0.35})^{B}(Ca_{1.83}Na_{0.11}Fe^{2+}_{0.05}Mn_{0.01})^{C}(Mg_{3.12}Fe^{2+}_{0.92}Al_{0.62}Ti_{0.25}Fe^{3+}_{0.10}V_{0.01})^{T}(Si_{5.97}Al_{2.03})^{V}O_{22}{}^{W}[(OH)_{1.99}F_{0.01}]_2$. Forsterite crystals have vitreous lustre with greenish to dark yellow colour, reaching up to 16 mm in size. Its chemical composition corresponds to the average endmember formula (n = 15) as $Fo_{88.9}Fa_{12.6}Tep_{0.2}$. This find represents an occurrence of unusually large crystals of pargasite associated with forsterite in igneous rocks of the Neogene Poľana stratovolcano.

Key words: *pargasite, forsterite, chemical composition, Očová, Poľana stratovolcano*

Received 10. 4. 2025; accepted 2. 6. 2025

Introduction

Pargasite occurs in a wide range of metamorphic and igneous rocks. Historically, it has been rarely described in Slovakia, reported only from andesites, basalts and other mafic to ultramafic rocks and their metamorphic equivalents from localities such as Fintice, Dobšiná, Fiľakovo and Brezno (Koděra et al. 1986 - 1990). Recently, however, more research has focused on these rare mineral occurrences discussed below (Huraiová et al. 1996; 2018; Hurai et al. 2007; Spišiak et al. 2021; 2022; Šimon et al. 2023 etc.). A new occurrence of pargasite and forsterite phenocrysts was recently discovered in the northwestern part of the Očová village. This article provides new chemical data on these minerals and describes another unusually large crystals at a new occurrence near the Poľana stratovolcano.

Localization and geological settings

The wider area of the studied occurrence lies within the Neogene (Lower - Middle Sarmatian) volcanic complex of the Poľana stratovolcano, specifically in the upper effusive Veľká Detva Formation and the lower Abčina Formation. The Veľká Detva Formation is composed of lava flows up to 100 m thick. It consists of medium-grained, porous dark grey to black andesite, composed of plagioclase, enstatite-ferrosilite, augite, amphibole, olivine and opaque minerals. Olivine phenocrysts reach sizes up to 0.3 mm. Only the Kalamárka lava flow differs from other flows by its higher olivine content (up to 1.1 vol. %) and the prevalent augite composition of pyroxenes over entatite-ferrosilite. Coarse to blocky epiclastic volcanic breccias and conglomerates of intermediate andesites of the Abčina Formation occur along the lava flow margins. These breccias contain fragments and blocks (20 - 80 cm in size) of fine-grained pyroxene to amphibole-pyroxene andesite (Dublan et al. 1997). The entire area is overlain by Pleistocene-Holocene deluvial and eluvial sediments, within which andesite and basalt boulders can be found. These rocks are often hydrothermally altered and contain carbonates or hyalite.

In previous years, the area was used as cultivated agricultural land, where loose pargasite crystals up to 6 × 3 cm were found. More recently, specimens were recovered by one of the authors (TB) from boulders piled along the forest edge, removed from the former field (Fig. 1). The locality lies approximately 500 m northwest of Lužno Hill (495 m a.s.l.) in the Brezina area near the village of Očová, Zvolen district, Banská Bystrica Region, central Slovakia. GPS coordinates are: 48°37’10.6”N 19°16’30.5”E.

Methods

Polished thin section of basalt sample was investigated using a polarised optical microscope Leica DM2500P (Department of Mineralogy, Petrology and Economic Geology, Faculty of Natural Sciences, Comenius University, Bratislava).

Quantitative chemical (WDS) analyses of studied minerals were obtained using a JEOL-JXA850F field-emission electron microprobe (EPMA) in wavelength-

-dispersive spectrometry (WDS) mode (Earth Science Institute, Slovak Academy of Sciences, Banská Bystrica, Slovakia). The following conditions were applied: accelerating voltage 15 kV, measuring current 20 nA. The beam diameter ranged from 5 to 10 μm, ZAF correction was used. The following standards and X-ray lines were used: albite (Al*Kα*, Na*Kα*), Cr_2O_3 (Cr*Kα*), Co (Co*Kα*), diopside (Si*Kα*, Mg*Kα*, Ca*Kα*), fluorapatite (P*Kα*), fluorite (F*Kα*), hematite (Fe*Kα*), Ni_2Si (Ni*Kα*), orthoclase (K*Kα*), rhodonite (Mn*Kα*), rutile (Ti*Kα*), $ScVO_4$ (V*Kα*) and tugtupite (Cl*Kα*). The detection limit of every element ranged from 0.02 to 0.03 wt.%. Elements which were analysed quantitatively and are below the detection limit are not listed in the tables. Used abbreviations of minerals are listed in Warr (2021).

Results

Pargasite and forsterite crystals occur in angular to subangular fragments of dark black vesicular basalts. Microscopically, these basalts exhibit a groundmass composed of glass and tabular basic plagioclase phenocrysts arranged in the intergranular spaces. It mostly contains idiomorphic to hypidiomorphic phenocrysts of olivine and orthopyroxenes, rarely clinopyroxene, which might be partially altered along the edges.

Forsterite crystals reach size up to 16 mm, they have vitreous lustre with greenish to dark yellow colour (Fig. 2). In BSE images, forsterite shows no chemical zoning (Fig. 4a). The chemical composition is homogenous with dominant Mg content (up to 1.77 *apfu*) and minor Fe^{2+} (up to 0.25 *apfu*) and Mn^{2+} (up to 0.01 *apfu*), corresponding to an average endmember formula (n = 15) $Fo_{88.9}Fa_{12.6}Tep_{0.2}$. Other constituents are below 0.01 *apfu* (Tab. 1).

Pargasite is common mineral found as vitreous dark brown to black crystals embedded in rocks in size up to 6 cm (Fig. 3). In BSE images, pargasite shows no chemical zoning (Fig. 4b). Amphibole is classified based on classification diagram (Fig. 5) suggested by Hawthorne et al. (2012). The chemical composition is stable at the position *T* fully occupied by Si (5.92 - 6.03 *apfu*) and Al (1.97 - 2.08 *apfu*). At the *C* site, Mg^{2+} (3.07 - 3.16 *apfu*) is

Fig. 1 *Mixed basalt and andesite boulders piled along the forest edge, removed from a nearby former field. Photo by P. Myšľan.*

Fig. 2 *Macrophotograph of representative sample of forsterite, sample size is 4.5 × 3 cm, crystal size is 1.0 × 0.5 cm. Photo by T. Bancík.*

Fig. 3 *Macrophotograph of representative sample of pargasite, sample size is 9 × 6 cm, crystal size is 2.5 × 1.5 cm. Photo by T. Bancík.*

dominant followed by Fe^{2+} (0.84 - 1.00 *apfu*). Mg#, calculated as $^{C}Mg/(Mg+Fe)$, ranges from 0.76 to 0.79. The content of Al^{3+} reaches up to 0.66 *apfu,* Fe^{3+} up to 0.15 *apfu* with Ti^{4+} in the range of 0.22 - 0.27 *apfu*. Because of its slightly elevated Ti content, the mineral composition projects into the pargasite and Ti-rich pargasite fields (Fig. 6) according to Hawthorne and Oberti (2006). At the *B* site, Ca (1.76 - 1.86 *apfu*) is dominant, with minor Na (up to 0.16 *apfu*), Fe^{2+} (up to 0.07 *apfu*) and Mn^{2+} (up to 0.02 *apfu*). The *A* site is dominated by Na^{+} (0.52 - 0.61 *apfu*) over K^{+} (0.33 - 0.36 *apfu*). The *W* site mostly contains $(OH)^{-}$, with only minor F^{-} (up to 0.03 *apfu*) and Cl^{-} (up to 0.01 *apfu*) (Tab. 2). The average crystallochemical formula (n = 15) corresponds to $^{A}(Na_{0.58}K_{0.35})^{B}(Ca_{1.83}Na_{0.11}Fe^{2+}_{0.05}Mn_{0.01})^{C}(Mg_{3.12}Fe^{2+}_{0.92}Al_{0.62}Ti_{0.25}Fe^{3+}_{0.10}V_{0.01})^{T}(Si_{5.97}Al_{2.03})^{V}O_{22}{}^{W}[(OH)_{1.99}F_{0.01}]_{2}$.

Minerals are sometimes found in the vugs overgrown by hyalite. The bigger vugs close to the surface tend to be open and minerals altered along the edges.

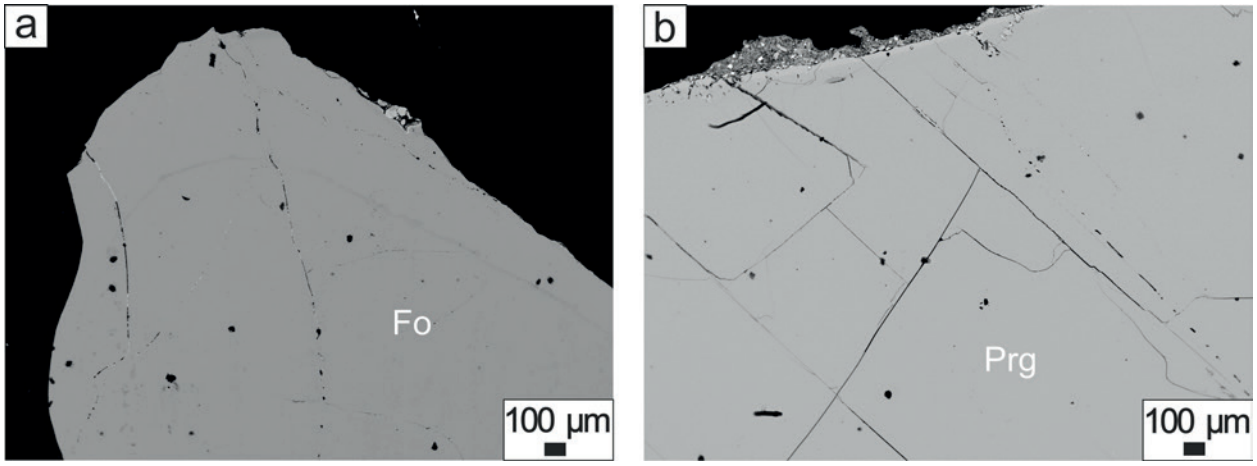

Fig. 4 *BSE images of* ***a)*** *forsterite and* ***b)*** *pargasite from Očová. Photo by T. Mikuš.*

Table 1 *Chemical composition of forsterite (wt. %) with calculated formulae on the basis of sum 3 cations (apfu) from Očová*

Analysis	1	2	3	4	5	6	7	8	9	10	11	12	13	14	15
SiO_2	39.67	40.27	39.77	39.54	39.47	39.36	39.72	39.82	39.62	39.81	40.05	39.52	39.62	39.47	39.54
TiO_2	0.00	0.00	0.07	0.00	0.00	0.00	0.16	0.04	0.00	0.03	0.00	0.00	0.00	0.00	0.00
Al_2O_3	0.07	0.04	0.00	0.04	0.05	0.03	0.00	0.05	0.00	0.03	0.00	0.00	0.00	0.06	0.04
Cr_2O_3	0.03	0.00	0.00	0.01	0.00	0.00	0.00	0.02	0.01	0.03	0.03	0.00	0.00	0.00	0.00
V_2O_3	0.00	0.00	0.00	0.00	0.00	0.00	0.00	0.00	0.03	0.05	0.00	0.04	0.00	0.04	0.00
FeO	11.64	12.02	11.67	11.68	11.75	11.84	12.29	11.92	10.34	11.69	11.81	11.52	11.82	11.96	12.07
MgO	47.68	48.06	47.68	47.50	47.84	47.24	47.71	47.82	47.33	47.71	47.71	47.78	47.76	47.68	47.17
MnO	0.09	0.20	0.16	0.13	0.17	0.18	0.17	0.22	0.17	0.14	0.08	0.16	0.15	0.17	0.16
NiO	0.11	0.15	0.10	0.14	0.12	0.23	0.11	0.32	0.19	0.23	0.23	0.22	0.22	0.13	0.13
CaO	0.13	0.15	0.14	0.14	0.11	0.15	0.13	0.14	0.15	0.13	0.12	0.15	0.15	0.17	0.17
Na_2O	0.00	0.02	0.00	0.06	0.04	0.00	0.00	0.04	0.02	0.00	0.00	0.00	0.00	0.07	0.03
K_2O	0.00	0.00	0.00	0.01	0.00	0.00	0.00	0.01	0.00	0.00	0.01	0.00	0.02	0.02	0.01
Total	99.42	100.90	99.59	99.26	99.56	99.02	100.30	100.40	97.86	99.83	100.04	99.40	99.74	99.76	99.32
Si	0.984	0.986	0.986	0.983	0.978	0.982	0.980	0.980	0.996	0.985	0.989	0.981	0.981	0.977	0.984
Ti	0.000	0.000	0.001	0.000	0.000	0.000	0.003	0.001	0.000	0.001	0.000	0.000	0.000	0.000	0.000
Al	0.002	0.001	0.000	0.001	0.002	0.001	0.000	0.002	0.000	0.001	0.000	0.000	0.000	0.002	0.001
Cr	0.001	0.000	0.000	0.000	0.000	0.000	0.000	0.000	0.000	0.001	0.001	0.000	0.000	0.000	0.000
V	0.000	0.000	0.000	0.000	0.000	0.000	0.000	0.000	0.001	0.001	0.000	0.001	0.000	0.001	0.000
Fe^{2+}	0.241	0.246	0.242	0.243	0.243	0.247	0.254	0.245	0.217	0.242	0.244	0.239	0.245	0.248	0.251
Mg	1.764	1.755	1.762	1.760	1.767	1.757	1.754	1.755	1.773	1.760	1.757	1.767	1.763	1.759	1.751
Mn	0.002	0.004	0.003	0.003	0.003	0.004	0.004	0.005	0.004	0.003	0.002	0.003	0.003	0.004	0.003
Ni	0.002	0.003	0.002	0.003	0.002	0.005	0.002	0.006	0.004	0.005	0.005	0.004	0.004	0.003	0.003
Ca	0.003	0.004	0.004	0.004	0.003	0.004	0.004	0.004	0.004	0.003	0.003	0.004	0.004	0.005	0.004
Na	0.000	0.001	0.000	0.003	0.002	0.000	0.000	0.002	0.001	0.000	0.000	0.000	0.000	0.003	0.001
K	0.000	0.000	0.000	0.000	0.000	0.000	0.000	0.000	0.000	0.000	0.000	0.000	0.001	0.001	0.000
Sum cat.	3.000	3.000	3.000	3.000	3.000	3.000	3.000	3.000	3.000	3.000	3.000	3.000	3.000	3.000	3.000
Fayalite	12.03	12.28	12.05	12.11	12.09	12.30	12.60	12.24	10.90	12.06	12.18	11.89	12.18	12.31	12.53
Forsterite	87.88	87.52	87.79	87.75	87.74	87.51	87.22	87.54	88.92	87.79	87.73	87.94	87.67	87.51	87.30
Tephroite	0.09	0.20	0.16	0.14	0.17	0.19	0.18	0.23	0.18	0.15	0.09	0.17	0.15	0.18	0.17

Discussion

Pargasite from igneous rocks has been rarely studied using modern analytical (chemical) methods. It mostly forms a series with kaersutite, having ^{C}Ti > 0.50 *apfu* and ^{W}O > 1.0 *apfu* (Hawthorne et al. 2012). Kaersutite is studied more frequently, it is predominantly found in alkaline basalts/basanites, where it forms phenocrysts. Kaersutite has also been identified to crystallize from melts affected by xenolith assimilation (Spišiak and Hovorka 1997). Huraiová et al. (1996) described a phase identified as Fe-Ti rich pargasite to kaersutite, with Ti in the range of 0.44 to 0.72 *apfu,* from mafic xenoliths composed predominantly of hornblende, clinopyroxene and forsterite Fo_{73-75} in Late Tertiary alkaline basalts near Pinciná in the Cerová vrchovina Highlands. Forsterite forms euhedral crystals with corroded grain margins, partly replaced by Fe, Ca, Mg, Mn- bearing hydroxides and carbonates. Kaersutite was also identified in tuffs of the maar near Gemerské Dechtáre village in an assemblage with spinel, feldspar and apatite. Megacrysts of kaersutite, with crystals up to 8 cm in size, associated with plagioclase, were found near Mašková (Huraiová et al. 2018). Kaersutite with forsterite were also described in the sandy filling of the Hajnáčka maar structure, associated with other heavy minerals including forsterite (Uher et al. 1999). It was also found as the megacryst assemblage in the Hajnáčka diatreme (Huraiová et al. 2018). On the other hand, pargasite amphiboles were

Table 2 *Chemical composition of pargasite (wt. %) with calculated formulae based on 24 (O,OH,F,Cl) (apfu) from Očová. Symbol * represents calculation of Fe_2O_3 from charge balance, ** represents calculation of H_2O from $(OH)^-$, Fe# calculated as $Fe^{3+}/(Fe^{3+}+Fe^{2+})$*

Analysis	1	2	3	4	5	6	7	8	9	10	11	12	13	14	15
SiO_2	40.27	40.38	39.83	39.93	40.29	40.14	40.34	39.89	40.07	40.47	40.07	40.16	40.17	39.80	40.23
TiO_2	1.94	1.96	2.11	2.16	2.28	2.35	2.15	2.15	2.22	2.16	2.45	2.30	2.11	2.35	2.20
Al_2O_3	15.30	14.90	15.07	15.09	14.91	15.04	15.19	14.99	15.33	15.08	15.12	15.05	14.86	15.37	15.09
V_2O_3	0.09	0.07	0.06	0.05	0.09	0.06	0.09	0.00	0.05	0.05	0.03	0.08	0.07	0.06	0.00
Cr_2O_3	0.00	0.06	0.01	0.00	0.03	0.00	0.00	0.00	0.00	0.03	0.04	0.00	0.04	0.00	0.00
Fe_2O_3*	0.84	0.36	1.20	1.27	0.90	1.32	0.96	0.96	1.23	0.70	0.93	0.31	0.84	0.92	1.15
FeO	7.79	8.08	7.67	7.51	7.81	7.36	7.63	7.57	7.54	7.57	7.94	7.83	7.54	7.80	7.76
MgO	14.06	13.79	14.17	14.24	14.02	14.00	14.20	14.08	14.20	14.27	13.99	13.93	14.08	13.96	14.08
MnO	0.17	0.07	0.09	0.15	0.07	0.09	0.05	0.14	0.12	0.13	0.13	0.03	0.15	0.04	0.07
CaO	11.59	11.50	11.61	11.47	11.37	11.60	11.49	11.48	11.47	11.59	11.54	11.66	11.48	11.49	11.48
Na_2O	2.48	2.52	2.30	2.37	2.43	2.33	2.41	2.36	2.36	2.41	2.32	2.41	2.39	2.44	2.28
K_2O	1.88	1.86	1.80	1.84	1.84	1.85	1.88	1.83	1.87	1.86	1.84	1.81	1.75	1.82	1.81
H_2O**	2.02	2.00	1.99	2.01	1.99	2.01	1.99	1.98	2.00	2.00	1.99	2.00	2.00	2.01	1.99
F	0.00	0.00	0.03	0.00	0.03	0.00	0.06	0.03	0.04	0.05	0.05	0.00	0.00	0.00	0.05
Cl	0.00	0.02	0.00	0.00	0.02	0.02	0.02	0.02	0.02	0.00	0.02	0.02	0.02	0.02	0.02
O=F,Cl	0.00	0.00	-0.01	0.00	-0.02	-0.01	-0.03	-0.01	-0.02	-0.02	-0.03	0.00	0.00	0.00	-0.03
Total	98.42	97.57	97.95	98.10	98.07	97.57	98.43	97.47	98.50	98.23	98.32	97.58	97.50	98.08	98.18
Si	5.968	6.033	5.935	5.938	5.989	5.983	5.971	5.966	5.931	5.994	5.946	5.992	5.998	5.92	5.972
Al	2.032	1.967	2.065	2.062	2.011	2.017	2.029	2.034	2.069	2.006	2.054	2.008	2.002	2.080	2.028
Sum *T*	8.000	8.000	8.000	8.000	8.000	8.000	8.000	8.000	8.000	8.000	8.000	8.000	8.000	8.000	8.000
Ti	0.216	0.220	0.237	0.242	0.255	0.264	0.239	0.242	0.247	0.241	0.274	0.258	0.237	0.263	0.246
Al	0.640	0.657	0.581	0.582	0.601	0.626	0.641	0.608	0.606	0.626	0.591	0.639	0.614	0.615	0.612
V	0.011	0.008	0.007	0.006	0.011	0.007	0.010	0.000	0.006	0.006	0.004	0.010	0.008	0.007	0.000
Cr	0.000	0.007	0.001	0.000	0.004	0.000	0.000	0.000	0.000	0.004	0.005	0.000	0.005	0.000	0.000
Fe^{3+}	0.094	0.041	0.135	0.142	0.101	0.148	0.107	0.107	0.137	0.078	0.104	0.034	0.094	0.103	0.128
Fe^{2+}	0.933	0.995	0.890	0.872	0.929	0.844	0.969	0.903	0.870	0.895	0.929	0.991	0.907	0.917	0.899
Mg	3.106	3.072	3.149	3.157	3.107	3.111	3.140	3.139	3.133	3.151	3.095	3.098	3.134	3.096	3.116
Sum *C*	5.000	5.000	5.000	5.001	5.002	5.000	4.999	4.999	4.999	5.001	5.002	5.000	4.999	5.001	5.001
Mn	0.021	0.009	0.011	0.019	0.009	0.011	0.006	0.018	0.015	0.002	0.002	0.004	0.019	0.005	0.009
Fe^{2+}	0.032	0.014	0.066	0.062	0.048	0.073	0.055	0.043	0.063	0.043	0.057	0.016	0.035	0.054	0.064
Ca	1.840	1.841	1.854	1.827	1.811	1.757	1.822	1.840	1.819	1.839	1.835	1.864	1.837	1.831	1.826
Na	0.106	0.136	0.070	0.092	0.132	0.158	0.117	0.099	0.103	0.116	0.106	0.116	0.110	0.110	0.101
Sum *B*	1.999	2.000	2.001	2.000	2.000	1.999	2.000	2.000	2.000	2.000	2.000	2.000	2.001	2.000	2.000
Na	0.606	0.594	0.595	0.592	0.568	0.515	0.575	0.585	0.575	0.576	0.561	0.581	0.582	0.594	0.555
K	0.355	0.355	0.342	0.349	0.349	0.352	0.355	0.349	0.353	0.351	0.348	0.345	0.333	0.345	0.343
Sum *A*	0.961	0.949	0.937	0.944	0.917	0.867	0.930	0.934	0.928	0.927	0.909	0.926	0.915	0.939	0.898
(OH)	2.000	1.995	1.986	2.000	1.981	1.995	1.967	1.981	1.976	1.977	1.972	1.995	1.995	1.995	1.971
F	0.000	0.000	0.014	0.000	0.014	0.000	0.028	0.014	0.019	0.023	0.023	0.000	0.000	0.000	0.023
Cl	0.000	0.005	0.000	0.000	0.005	0.005	0.005	0.005	0.005	0.000	0.005	0.005	0.005	0.005	0.005
Sum *W*	2.000	2.000	2.000	2.000	2.000	2.000	2.000	2.001	1.999	2.000	2.001	2.000	2.000	2.000	2.000
Sum cat.	15.994	15.962	15.982	15.990	15.952	15.947	15.967	15.972	15.974	15.957	15.949	15.937	15.950	15.974	15.941
Fe#	0.09	0.04	0.13	0.14	0.10	0.15	0.10	0.11	0.14	0.08	0.10	0.03	0.09	0.10	0.12

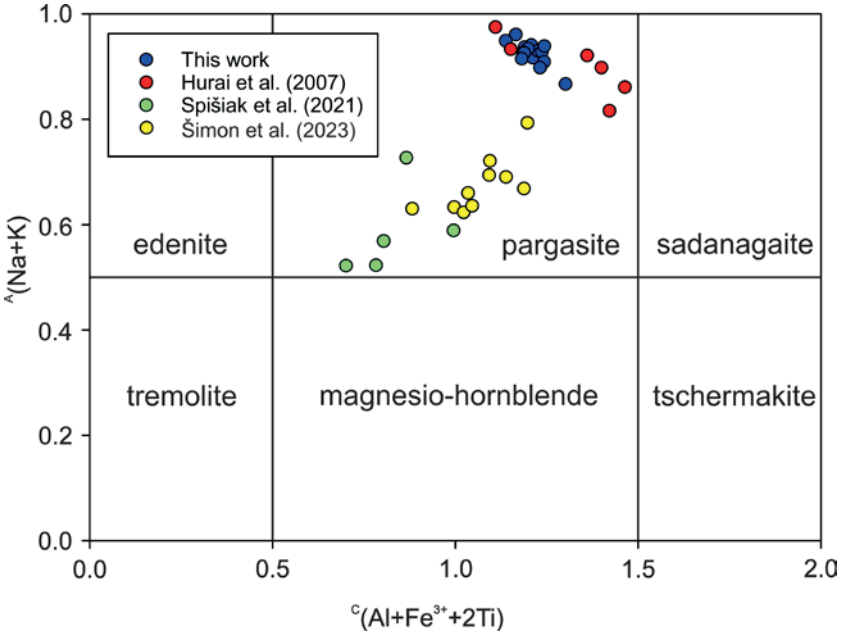

Fig. 5 *Classification diagram (Hawthorne et al. 2012) for calcium amphiboles and their compositional boundaries with representative analyses of pargasite from Očová.*

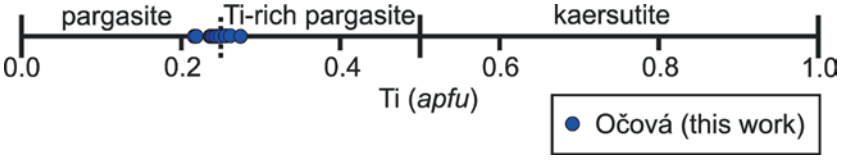

Fig. 6 *Compositional variation diagram for pargasite-kaersutite based on Ti (apfu) content (modified after Hawthorne and Oberti 2006) for amphiboles from Očová.*

confirmed as slightly zonal anhedral to subhedral crystals in andesites from the Neogene volcanics of the Burda Mountains (Šimon et al. 2023). Furthermore, pargasite was identified in strongly altered basic to intermediate volcanic rocks from the Permian Hronic Unit, associated with clinopyroxene, spinel, biotite and plagioclase (Spišiak et al. 2021). Potassic pargasite with ^{A}K >0.50 has also been reported from carbonatic pyroxenite xenoliths associated with diopside, fluorapatite, carbonates, phlogopite, spinel, albite and feldspars, occurring in ultrapotassic dacite-trachydacite glass from alkali basalts in the Cerová vrchovina Highland (Hurai et al. 2007). Generally, the higher Ti content from igneous pargasite occurrences is similar to the Ti-rich pargasite studied from Očová, with increased Ti up to 0.27 *apfu* (Fig. 4). Studied pargasite shows low $Fe^{3+}/(Fe^{3+}+Fe^{2+})$ ratio (less than 0.15) with increased Ti content and relatively low sums, indicating the presence of oxy-component (O^{2-} in the *W*-site), similar to other Ti-rich amphiboles such as pargasite or kaersutite from other occurrences (e.g. Satoh et al. 2004).

The composition of olivine phenocrysts is similar to those from other alkali basalts and their xenoliths in Cerová vrchovina Highland. (Huraiová 1996; Uher et al. 1999; Reato et al. 2022, etc.). Studied forsterite similarly shows minimal or no zoning in BSE. Forsterite from Ostrá Lúka basalts displays sharp boundaries with core and rim, where core has the highest Fo_{85} component and lower forsterite component (up to 65 mol.%) was observed along the edges (Spišiak et al. 2022).

Conclusions

A new occurrence of pargasite and forsterite phenocrysts in basalts has been discovered in the northwestern part of the Očová village, Poľana Mountains, central Slovakia. This represents a new occurrence of unusually large crystals of pargasite and forsterite in igneous rocks.

Acknowledgment

The authors are thankful to reviewers Petr Gadas and Richard Kopáčik and handling editor Jiří Sejkora for their suggestions. Thanks also go to P. Sečkár for preparing the polished thin sections. This study was financially supported by the Slovak Research and Development Agency (project APVV-22-0041) and Scientific grant agency of the Ministry of Education, Research, Development and Youth of the Slovak Republic and the Slovak Academy of Sciences (VEGA 2/0029/23).

Literature

Dublan L (Ed.), Bezák V, Biely A, Bujovský A, Halouzka R, Hraško Ľ, Köhlerová M, Marcin D, Onačila D, Scherer S, Vozárová A, Vozár J, Žáková E (1997) Explanations to the geological map of Poľana 1:50 000. GSSR, Bratislava, 1-238

Hawthorne FC, Oberti R (2006) On the classification of amphiboles. Can Mineral 44(1): 1-21

Hawthorne FC, Oberti R, Harlow GE, Maresch WV, Martin RF, Schumacher JC, Welch MD (2012) Nomenclature of the amphibole supergroup. Am Mineral 97: 2031-2048

Hurai V, Huraiová M, Konečný P, Thomas R (2007) Mineral-melt-fluid composition of carbonate-bearing cumulate xenoliths in Tertiary alkali basalts of southern Slovakia. Mineral Mag 71(1): 63-79

Huraiová M, Konečný P, Konečný V, Simon K, Hurai V (1996) Mafic and salic igneous xenoliths in late Tertiary alkaline basalts; fluid inclusion and mineralogical evidence for a deep-crustal magmatic reservoir in the Western Carpathians. Eur J Mineral 8(5): 901-916

Huraiová M, Lengauer CL, Abart R, Hurai V (2018) Compositional, structural and vibrational spectroscopic characteristics of feldspar megacrysts in alkali basalts from southern Slovakia. J Geo Sci 63: 215-226

Koděra M, Andrusovová-Vlčeková G, Belešová O, Briatková D, Dávidová Š, Fejdiová V, Hurai V, Chovan M, Nelišerová E, Ženiš P (1986-1990) Topographic mineralogy of Slovakia. I-III. Veda, Bratislava, 1-1592 (in Slovak)

Reato L, Huraiová M, Konečný P, Marko F, Hurai V (2022) Formation of eseneite and kushiroite in tschermakite-bearing calc-silicate xenoliths ejected in alkali basalt. Minerals 12(2): 156

Satoh H, Yamaguchi YY, Makino K (2004) Ti-substitution mechanism in plutonic oxy-kaersutite from the Larvik alkaline complex, Oslo rift, Norway. Mineral Mag 68(4): 687-697

Spišiak J, Hovorka D (1997) Petrology of the Western Carpathians Cretaceous primitive alkaline volcanics. Geol Carpath 48(2): 113-121

Spišiak J, Prokešová R, Butek J, Šimonová V (2022) Neogene alkali basalts from Central Slovakia (Ostrá Lúka lava complex); mineralogy and geochemistry. Minerals 12(2): 195

Spišiak J, Vozárová A, Vozár J, Ferenc Š, Šimonová V, Butek J (2021) Implication of mineralogy and isotope data on the origin of the Permian basic volcanic rocks of the Hronicum (Slovakia, Western Carpathians). Minerals 11(8): 841

Šimon L, Kollárová V, Kováčiková M (2023) Neogene volcanics of the Burda mountain range nearby Štúrovo, Slovakia. Mineral Slov 55(2): 117-132

Uher P, Sabol M, Konečný P, Gregáňová M, Táborský Z, Puškelová Ľ (1999) Sapphire from Hajnáčka (Cerová Highland, southern Slovakia). Slovak Geol Mag 5: 273-280

Warr LN (2021) IMA-CNMNC approved mineral symbols. Mineral Mag 85: 291-320